

Single-boson exchange fRG and its application to the Hubbard model

Kilian Fraboulet

Institut für Theoretische Physik and Center for Quantum Science, Universität Tübingen



Functional Methods in Strongly Correlated Systems (FunSCS2023)

September 13, 2023

In collaboration with:

Aiman Al-Eryani (Ruhr-Universität Bochum)

Sarah Heinzelmann (Universität Tübingen)

Sabine Andergassen (Technische Universität Wien)

Alessandro Toschi (Technische Universität Wien)

Pietro M. Bonetti (Max-Planck-Institute Stuttgart)

Demetrio Vilardi (Max-Planck-Institute Stuttgart)

1 Single-boson exchange fRG

- SBE formalism
- SBE fRG formalism
- Application to the Hubbard model

2 Extension to strong couplings using DMF²RG

- Merits of fRG with correlated starting point
- Application to the Hubbard model

Single-boson exchange fRG

Section based on:

KF, S. Heinzelmann, P.M. Bonetti, A. Al-Eryani, D. Vilaridi, A. Toschi, and S. Andergassen, SBE fRG application to the 2D Hubbard model at weak coupling, Eur. Phys. J. B 95, 202 (2022)

Consider a fermionic theory with a quartic interaction:

$$S[\bar{\psi}, \psi] = - \sum_{\alpha_1, \alpha_2} \bar{\psi}_{\alpha_1} G_{0, \alpha_1 | \alpha_2}^{-1} \psi_{\alpha_2} + \sum_{\alpha_1, \alpha_2, \alpha_3, \alpha_4} U_{\alpha_1 \alpha_2 | \alpha_3 \alpha_4} \bar{\psi}_{\alpha_1} \bar{\psi}_{\alpha_2} \psi_{\alpha_3} \psi_{\alpha_4}$$

Consider a fermionic theory with a quartic interaction:

$$S[\bar{\psi}, \psi] = - \sum_{\alpha_1, \alpha_2} \bar{\psi}_{\alpha_1} G_{0, \alpha_1 | \alpha_2}^{-1} \psi_{\alpha_2} + \sum_{\alpha_1, \alpha_2, \alpha_3, \alpha_4} U_{\alpha_1 \alpha_2 | \alpha_3 \alpha_4} \bar{\psi}_{\alpha_1} \bar{\psi}_{\alpha_2} \psi_{\alpha_3} \psi_{\alpha_4}$$

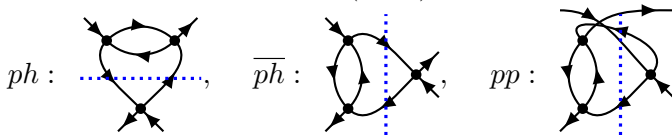
2P-reducibility vs U -reducibility:

Consider a fermionic theory with a quartic interaction:

$$S[\bar{\psi}, \psi] = - \sum_{\alpha_1, \alpha_2} \bar{\psi}_{\alpha_1} G_{0, \alpha_1 | \alpha_2}^{-1} \psi_{\alpha_2} + \sum_{\alpha_1, \alpha_2, \alpha_3, \alpha_4} U_{\alpha_1 \alpha_2 | \alpha_3 \alpha_4} \bar{\psi}_{\alpha_1} \bar{\psi}_{\alpha_2} \psi_{\alpha_3} \psi_{\alpha_4}$$

2P-reducibility vs U -reducibility:

- 2P-reducible diagram = diagram that can be disconnected after cutting two **propagator** lines ($\Leftrightarrow G$):

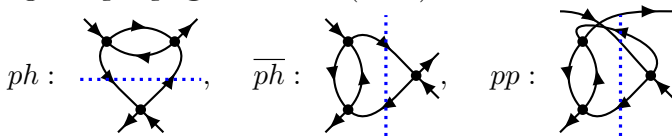


Consider a fermionic theory with a quartic interaction:

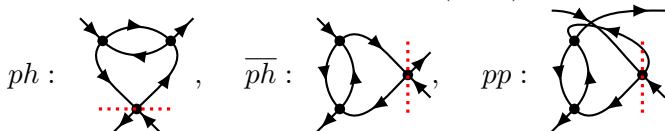
$$S[\bar{\psi}, \psi] = - \sum_{\alpha_1, \alpha_2} \bar{\psi}_{\alpha_1} G_{0, \alpha_1 | \alpha_2}^{-1} \psi_{\alpha_2} + \sum_{\alpha_1, \alpha_2, \alpha_3, \alpha_4} U_{\alpha_1 \alpha_2 | \alpha_3 \alpha_4} \bar{\psi}_{\alpha_1} \bar{\psi}_{\alpha_2} \psi_{\alpha_3} \psi_{\alpha_4}$$

2P-reducibility vs U -reducibility:

- 2P-reducible diagram = diagram that can be disconnected after cutting two **propagator lines** ($\Leftrightarrow G$):



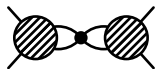
- U -reducible diagram = diagram that can be disconnected after cutting one **bare interaction vertex** ($\Leftrightarrow U$):



2P-reducibility vs U -reducibility:

2P-reducibility vs U -reducibility:

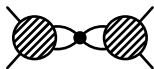
- Consider the general form of a U -reducible diagram:



U -reducibility \Rightarrow 2P-reducibility

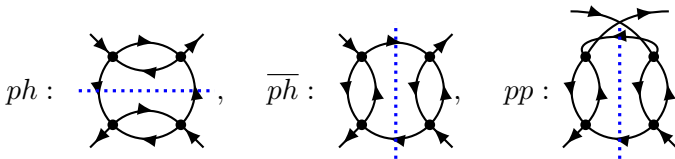
2P-reducibility vs U -reducibility:

- Consider the general form of a U -reducible diagram:



U -reducibility \Rightarrow 2P-reducibility

- Consider the following 2P-reducible diagrams:



2P-reducibility $\not\Rightarrow$ U -reducibility

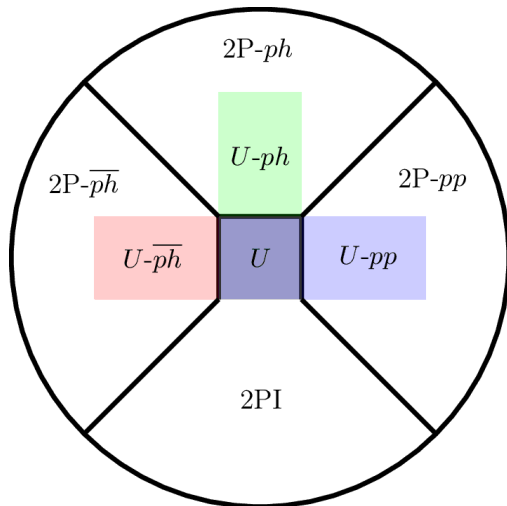
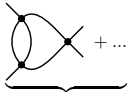


Figure adapted from Krien, Valli, Capone, PRB 100, 155149 (2019)

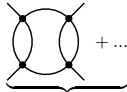
⇒ The class of 2P-reducible diagrams fully contains that of U -reducible diagrams

Single-boson exchange (SBE) decomposition (Krien, Valli, Capone, PRB 100, 155149 (2019)):

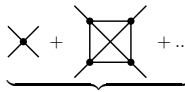
$$\Gamma^{(4)} = \frac{\delta^4 \Gamma[\bar{\psi}, \psi]}{\delta \bar{\psi} \delta \bar{\psi} \delta \psi \delta \psi} \Big|_{\psi = \bar{\psi} = 0} = \sum_{x=\{\text{pp, ph, p}\bar{\text{h}}\}} (\nabla^x + M^x - U) + \mathcal{I}^{2\text{PI}}$$

with $\nabla^x =$  + ...

only U -reducible graphs

$M^x =$  + ...

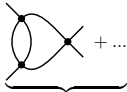
only U -irreducible and $2P$ -reducible graphs

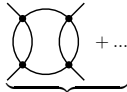
$\mathcal{I}^{2\text{PI}} =$  + ...

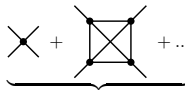
only 2PI graphs

Single-boson exchange (SBE) decomposition (Krien, Valli, Capone, PRB 100, 155149 (2019)):

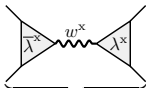
$$\Gamma^{(4)} = \frac{\delta^4 \Gamma[\bar{\psi}, \psi]}{\delta \bar{\psi} \delta \bar{\psi} \delta \psi \delta \psi} \Big|_{\psi = \bar{\psi} = 0} = \sum_{x=\{pp, ph, p\bar{h}\}} (\nabla^x + M^x - U) + \mathcal{I}^{2PI}$$

with $\nabla^x =$  + ...
 only U-reducible graphs

$M^x =$  + ...
 only U-irreducible and 2P-reducible graphs

$\mathcal{I}^{2PI} =$  + ...
 only 2PI graphs

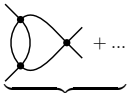
Heart of the SBE decomposition:

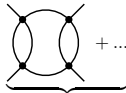
$\nabla^x =$ 
 1 boson exchanged

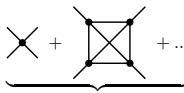
w : bosonic propagator
 λ : Yukawa coupling
 M : rest function

Single-boson exchange (SBE) decomposition (Krien, Valli, Capone, PRB 100, 155149 (2019)):

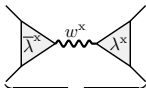
$$\Gamma^{(4)} = \frac{\delta^4 \Gamma[\bar{\psi}, \psi]}{\delta \bar{\psi} \delta \bar{\psi} \delta \psi \delta \psi} \Big|_{\psi = \bar{\psi} = 0} = \sum_{x=\{\text{pp,ph,ph}\}} (\nabla^x + M^x - U) + \mathcal{I}^{2\text{PI}}$$

with $\nabla^x =$  + ...
 only U-reducible graphs

$M^x =$  + ...
 only U-irreducible and 2P-reducible graphs

$\mathcal{I}^{2\text{PI}} =$  + ...
 only 2PI graphs

Heart of the SBE decomposition:

$\nabla^x =$ 
 1 boson exchanged

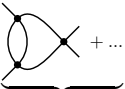
w : bosonic propagator
 λ : Yukawa coupling
 M : rest function

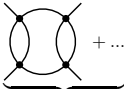
\Rightarrow Focus on translationally invariant and $SU(2)$ -spin-symmetric systems (see Gievers, Walter, Ge, von Delft, Kugler, EPJB 95, 108 (2022) for a more general formulation of the SBE decomposition):

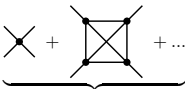
$$\nabla_{kk'}^x(Q) = \bar{\lambda}_k^x(Q) w^x(Q) \lambda_{k'}^x(Q) \quad k^{(\prime)} = (\mathbf{k}^{(\prime)}, \nu^{(\prime)}) \quad Q = (\mathbf{Q}, \Omega)$$

Single-boson exchange (SBE) decomposition (Krien, Valli, Capone, PRB 100, 155149 (2019)):

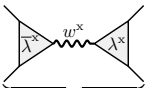
$$\Gamma^{(4)} = \frac{\delta^4 \Gamma[\bar{\psi}, \psi]}{\delta \bar{\psi} \delta \bar{\psi} \delta \psi \delta \psi} \Big|_{\psi = \bar{\psi} = 0} = \sum_{x=\{pp, ph, \bar{p}\bar{h}\}} (\nabla^x + M^x - U) + \mathcal{I}^{2PI}$$

with $\nabla^x =$  + ...
 only U-reducible graphs

$M^x =$  + ...
 only U-irreducible and 2P-reducible graphs

$\mathcal{I}^{2PI} =$  + ...
 only 2PI graphs

Heart of the SBE decomposition:

$\nabla^x =$ 
 1 boson exchanged

w : bosonic propagator
 λ : Yukawa coupling
 M : rest function

\Rightarrow Focus on translationally invariant and $SU(2)$ -spin-symmetric systems (see Gievers, Walter, Ge, von Delft, Kugler, EPJB 95, 108 (2022) for a more general formulation of the SBE decomposition):

$$\nabla_{kk'}^x(Q) = \bar{\lambda}_k^x(Q) w^x(Q) \lambda_{k'}^x(Q) \quad k^{(\prime)} = (\mathbf{k}^{(\prime)}, \nu^{(\prime)}) \quad Q = (\mathbf{Q}, \Omega)$$

\Rightarrow SBE decomposition introduces **bosonic dofs** and treats **all channels equitably**

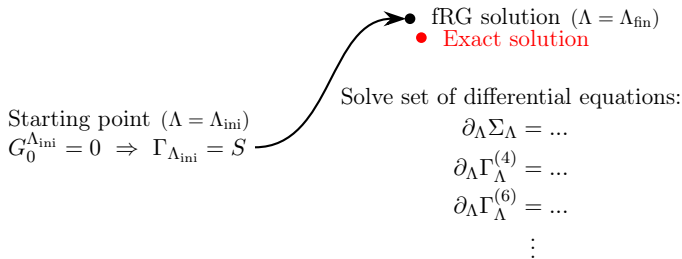
Functional renormalization group (fRG) in a nutshell (Wetterich, PLB 301, 90 (1993)):

$$\text{Introduce cutoff function: } G_0 \rightarrow G_0^\Lambda \Rightarrow \partial_\Lambda \Gamma_\Lambda = \text{[circle with slash]} \Rightarrow \begin{cases} \partial_\Lambda \Sigma_\Lambda = \dots \\ \partial_\Lambda \Gamma_\Lambda^{(4)} = \dots \\ \partial_\Lambda \Gamma_\Lambda^{(6)} = \dots \\ \vdots \end{cases}$$

Functional renormalization group (fRG) in a nutshell (Wetterich, PLB 301, 90 (1993)):

Introduce cutoff function: $G_0 \rightarrow G_0^\Lambda \Rightarrow \partial_\Lambda \Gamma_\Lambda = \text{circle with slash} \Rightarrow \begin{cases} \partial_\Lambda \Sigma_\Lambda = \dots \\ \partial_\Lambda \Gamma_\Lambda^{(4)} = \dots \\ \partial_\Lambda \Gamma_\Lambda^{(6)} = \dots \\ \vdots \end{cases}$

Illustration of the fRG flow:



fRG for fermionic systems typically relies on a **hierarchy of equations for the 1PI vertices** derived from a vertex expansion of the Wetterich equation:

$$\begin{aligned}
 \partial_\Lambda \Sigma_\Lambda &= \text{Diagram 1} \\
 \partial_\Lambda \Gamma_\Lambda^{(4)} &= \text{Diagram 2} + \text{Diagram 3} \\
 \partial_\Lambda \Gamma_\Lambda^{(6)} &= \dots \\
 &\quad \vdots
 \end{aligned}$$

Diagram 1: A square loop with a horizontal line across the top. The top-left and top-right corners are labeled G_Λ . The top horizontal line is labeled $\partial_\Lambda (G_0^\Lambda)^{-1}$. The bottom horizontal line is labeled $\Gamma_\Lambda^{(4)}$. Two external lines enter from the bottom.

Diagram 2: Two square loops connected by a horizontal line across their top edges. Each square loop has a horizontal line across its top edge and is labeled $\Gamma_\Lambda^{(4)}$ on its bottom edge. Two external lines enter from the bottom of each square.

Diagram 3: A hexagonal loop with a horizontal line across its top edge. The bottom horizontal line is labeled $\Gamma_\Lambda^{(6)}$. Two external lines enter from the bottom.

fRG for fermionic systems typically relies on a **hierarchy of equations for the 1PI vertices** derived from a vertex expansion of the Wetterich equation:

$$\partial_\Lambda \Sigma_\Lambda = \text{Diagram 1}$$

$$\partial_\Lambda \Gamma_\Lambda^{(4)} = \text{Diagram 2} + \text{Diagram 3}$$

$$\cancel{\partial_\Lambda \Gamma_\Lambda^{(6)}} = \dots$$

✘

⇒ Truncate in practice at level 2 (**1-loop truncation**)

fRG for fermionic systems typically relies on a **hierarchy of equations for the 1PI vertices** derived from a vertex expansion of the Wetterich equation:

$$\partial_\Lambda \Sigma_\Lambda = \text{Diagram 1}$$

$$\partial_\Lambda \Gamma_\Lambda^{(4)} = \text{Diagram 2} + \text{Diagram 3}$$

$$\cancel{\partial_\Lambda \Gamma_\Lambda^{(6)}} = \dots$$

✘

⇒ Truncate in practice at level 2 (**1-loop truncation**)

⚠ fRG approach **restricted to weak couplings** for fermionic systems

Inserting the SBE decomposition of $\Gamma^{(4)}$ into the flow equation $\partial_\Lambda \Gamma_\Lambda^{(4)} \equiv \partial_\Lambda \Gamma^{(4)} = \dots$ yields (Bonetti, Toschi, Hille, Andergassen, Vilardi, PRR 4, 013034 (2022)):

$$\begin{aligned}\partial_\Lambda w^X(Q) &= [w^X(Q)]^2 \int_p \lambda_p^X(Q) \left[\tilde{\partial}_\Lambda \Pi_p^X(Q) \right] \lambda_p^X(Q) \\ \partial_\Lambda \lambda_k^X(Q) &= \int_p \mathcal{I}_{kp}^X(Q) \left[\tilde{\partial}_\Lambda \Pi_p^X(Q) \right] \lambda_p^X(Q) \\ \partial_\Lambda M_{kk'}^X(Q) &= \int_p \mathcal{I}_{kp}^X(Q) \left[\tilde{\partial}_\Lambda \Pi_p^X(Q) \right] \mathcal{I}_{pk'}^X(Q)\end{aligned}$$

with $\mathcal{I}^X \sim \Gamma^{(4)} - \lambda^X w^X \lambda^X$, $\Pi^X \sim GG$, $\tilde{\partial}_\Lambda G = \partial_\Lambda G|_{\Sigma=\text{const}}$ and X physical channels (X = M, D, SC)

Inserting the SBE decomposition of $\Gamma^{(4)}$ into the flow equation $\partial_\Lambda \Gamma_\Lambda^{(4)} \equiv \partial_\Lambda \Gamma^{(4)} = \dots$ yields (Bonetti, Toschi, Hille, Andergassen, Vilardi, PRR 4, 013034 (2022)):

$$\begin{aligned}\partial_\Lambda w^X(Q) &= [w^X(Q)]^2 \int_p \lambda_p^X(Q) \left[\tilde{\partial}_\Lambda \Pi_p^X(Q) \right] \lambda_p^X(Q) \\ \partial_\Lambda \lambda_k^X(Q) &= \int_p \mathcal{I}_{kp}^X(Q) \left[\tilde{\partial}_\Lambda \Pi_p^X(Q) \right] \lambda_p^X(Q) \\ \partial_\Lambda M_{kk'}^X(Q) &= \int_p \mathcal{I}_{kp}^X(Q) \left[\tilde{\partial}_\Lambda \Pi_p^X(Q) \right] \mathcal{I}_{pk'}^X(Q)\end{aligned}$$

with $\mathcal{I}^X \sim \Gamma^{(4)} - \lambda^X w^X \lambda^X$, $\Pi^X \sim GG$, $\tilde{\partial}_\Lambda G = \partial_\Lambda G|_{\Sigma=\text{const}}$ and X physical channels (X = M, D, SC)

⚠ Still solve the flow equation for the self-energy $\partial_\Lambda \Sigma_\Lambda = \dots$ as in the conventional fermionic fRG:

$$\partial_\Lambda \Sigma(k) = \int_p \left[2\Gamma^{(4)}(k, k, p) - \Gamma^{(4)}(p, k, k) \right] \underbrace{\tilde{\partial}_\Lambda G(p)}_{S(p)}$$

Inserting the SBE decomposition of $\Gamma^{(4)}$ into the flow equation $\partial_\Lambda \Gamma_\Lambda^{(4)} \equiv \partial_\Lambda \Gamma^{(4)} = \dots$ yields (Bonetti, Toschi, Hille, Andergassen, Vilardi, PRR 4, 013034 (2022)):

$$\begin{aligned}\partial_\Lambda w^X(Q) &= [w^X(Q)]^2 \int_p \lambda_p^X(Q) \left[\tilde{\partial}_\Lambda \Pi_p^X(Q) \right] \lambda_p^X(Q) \\ \partial_\Lambda \lambda_k^X(Q) &= \int_p \mathcal{I}_{kp}^X(Q) \left[\tilde{\partial}_\Lambda \Pi_p^X(Q) \right] \lambda_p^X(Q) \\ \partial_\Lambda M_{kk'}^X(Q) &= \int_p \mathcal{I}_{kp}^X(Q) \left[\tilde{\partial}_\Lambda \Pi_p^X(Q) \right] \mathcal{I}_{pk'}^X(Q)\end{aligned}$$

with $\mathcal{I}^X \sim \Gamma^{(4)} - \lambda^X w^X \lambda^X$, $\Pi^X \sim GG$, $\tilde{\partial}_\Lambda G = \partial_\Lambda G|_{\Sigma=\text{const}}$ and X physical channels (X = M, D, SC)

⚠ Still solve the flow equation for the self-energy $\partial_\Lambda \Sigma_\Lambda = \dots$ as in the conventional fermionic fRG:

$$\partial_\Lambda \Sigma(k) = \int_p \left[2\Gamma^{(4)}(k, k, p) - \Gamma^{(4)}(p, k, k) \right] \underbrace{\tilde{\partial}_\Lambda G(p)}_{S(p)}$$

⚠ Still use the frequency-dependent cutoff:

$$G_0^\Lambda(\mathbf{k}, \nu) = \frac{\nu^2}{\nu^2 + \Lambda^2} G_0(\mathbf{k}, \nu) \quad \text{with } G_0^{\Lambda_{\text{ini}}=\infty} = 0$$

Illustration of the 1-loop SBE fRG flow:

Starting point ($\Lambda = \Lambda_{\text{ini}}$)

$$\Sigma_{\Lambda_{\text{ini}}} = 0, w_{\Lambda_{\text{ini}}}^X = U,$$

$$\lambda_{\Lambda_{\text{ini}}}^X = 1, M_{\Lambda_{\text{ini}}}^X = 0$$

Solve set of differential equations:

$$\partial_{\Lambda} \Sigma_{\Lambda} = \partial_{\Lambda} \Sigma_{\Lambda}^{(1)}$$

$$\partial_{\Lambda} w_{\Lambda}^X = \partial_{\Lambda} w_{\Lambda}^{X(1)}$$

$$\partial_{\Lambda} \lambda_{\Lambda}^X = \partial_{\Lambda} \lambda_{\Lambda}^{X(1)}$$

$$\left(\partial_{\Lambda} M_{\Lambda}^X = \partial_{\Lambda} M_{\Lambda}^{X(1)} \right)$$

fRG solution ($\Lambda = \Lambda_{\text{fin}}$)

• Exact solution

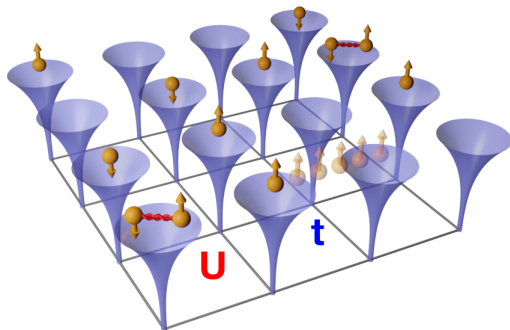


Figure taken from Qin, Schäfer, Andergassen, Corboz, Gull, ARCMP 13, 275 (2022)

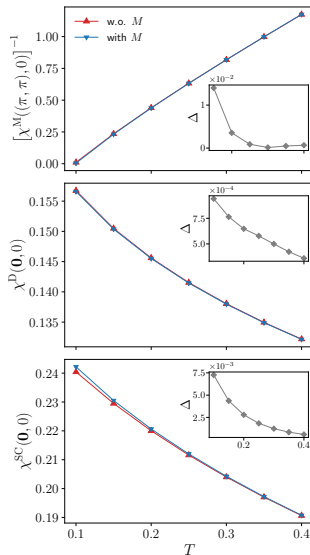
Chosen playground = 2D Hubbard model:

$$\mathcal{H} = \sum_{i \neq j, \sigma} t_{ij} c_{i\sigma}^\dagger c_{j\sigma} + U \sum_i c_{i\uparrow}^\dagger c_{i\uparrow} c_{i\downarrow}^\dagger c_{i\downarrow} - \mu \sum_{i,\sigma} c_{i\sigma}^\dagger c_{i\sigma}$$

- $t_{ij} = -t = -1$ for i, j nearest-neighbor sites (0 otherwise)
- $U =$ **on-site** Coulomb interaction

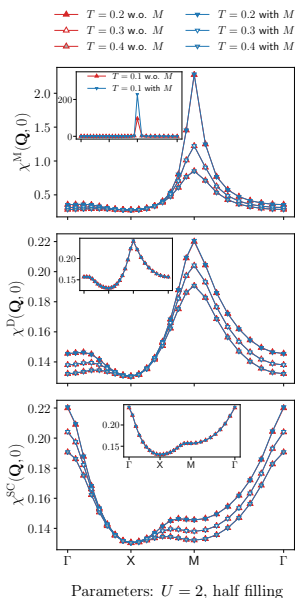
$$M = \text{Diagram} + \dots$$

M has **negligible** effects on physical observables
in **most** studied parameter regimes



⚠ Violation of Mermin-Wagner theorem
 observed with and without M

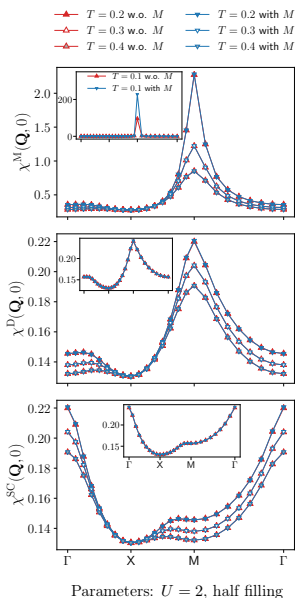
⇒ Pseudo-critical transition observed at half filling



⚠ Violation of Mermin-Wagner theorem
 observed with and without M

⇒ Pseudo-critical transition observed at half filling

↪ Feature inherent to our truncation of the fRG
 hierarchy but not to the SBE scheme

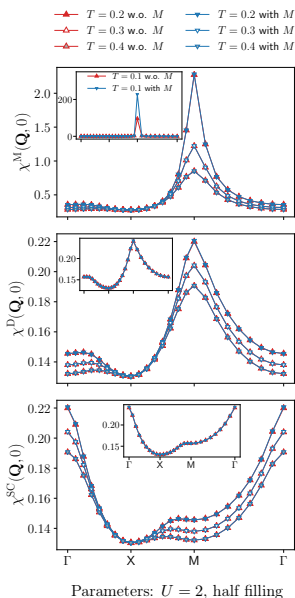


⚠ Violation of Mermin-Wagner theorem
 observed with and without M

⇒ Pseudo-critical transition observed at half filling

↪ Feature inherent to our truncation of the fRG
 hierarchy but not to the SBE scheme

What happens to the SBE quantities (w , λ , M)
 near the pseudo-critical transition?



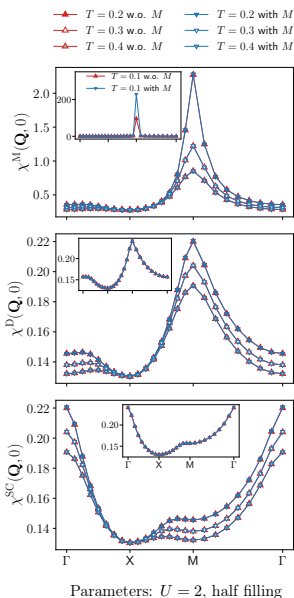
⚠ Violation of Mermin-Wagner theorem
 observed with and without M

⇒ Pseudo-critical transition observed at half filling

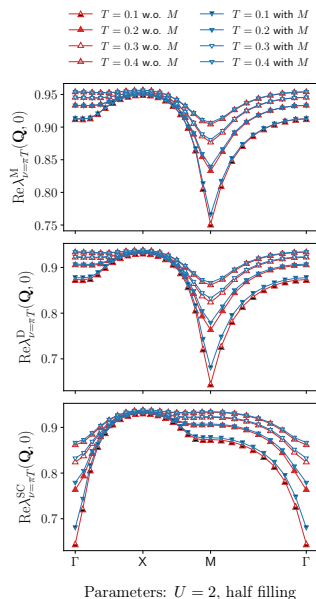
↔ Feature inherent to our truncation of the fRG
 hierarchy but not to the SBE scheme

What happens to the SBE quantities (w , λ , M)
 near the pseudo-critical transition?

⇒ w^M diverges ($w^X(Q) = U \pm U^2 \chi^X(Q)$)



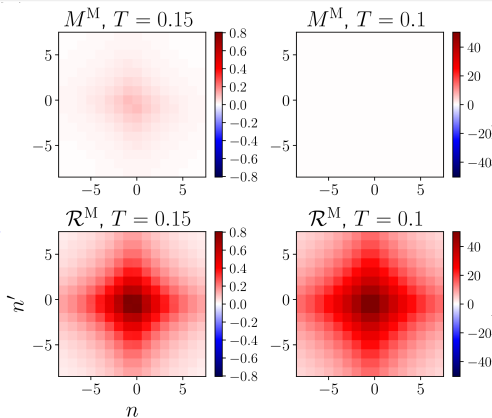
$\Rightarrow \lambda^M$ remains finite



$$\mathcal{R}_{kk'}^X(Q) = \phi_{kk'}^X(Q) - \mathcal{K}^{(1)X}(Q) - \mathcal{K}_k^{(2)X}(Q) - \mathcal{K}_{k'}^{(2)X}(Q)$$

$$\mathcal{K}^{(1)X}(Q) = \lim_{\nu, \nu' \rightarrow \infty} \phi_{(k, \nu), (k', \nu')}^X(Q)$$

$$\mathcal{K}_k^{(2)X}(Q) = \lim_{\nu' \rightarrow \infty} \phi_{k, (k', \nu')}^X(Q) - \mathcal{K}^{(1)X}(Q)$$



Results for $M_{\nu\nu'}^M((\pi, \pi), 0)$ and $\mathcal{R}_{\nu\nu'}^M((\pi, \pi), 0)$

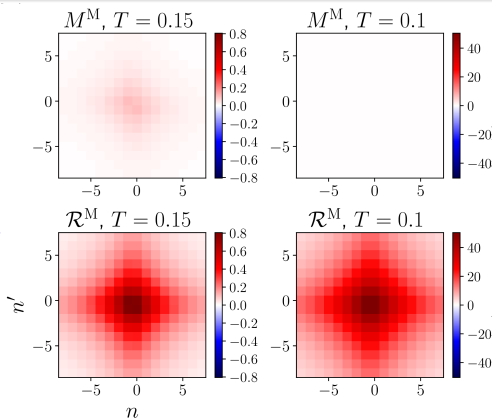
Parameters: $U = 2$, half filling

$\Rightarrow M^M$ remains finite

$$\mathcal{R}_{kk'}^X(Q) = \phi_{kk'}^X(Q) - \mathcal{K}^{(1)X}(Q) - \mathcal{K}_k^{(2)X}(Q) - \mathcal{K}_{k'}^{(2)X}(Q)$$

$$\mathcal{K}^{(1)X}(Q) = \lim_{\nu, \nu' \rightarrow \infty} \phi_{(k, \nu), (k', \nu')}^X(Q)$$

$$\mathcal{K}_k^{(2)X}(Q) = \lim_{\nu' \rightarrow \infty} \phi_{k, (k', \nu')}^X(Q) - \mathcal{K}^{(1)X}(Q)$$



Results for $M_{\nu\nu'}^M((\pi, \pi), 0)$ and $\mathcal{R}_{\nu\nu'}^M((\pi, \pi), 0)$

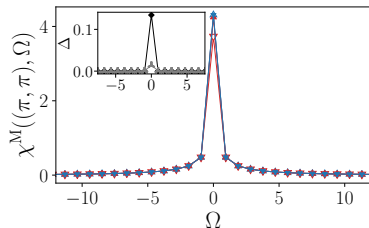
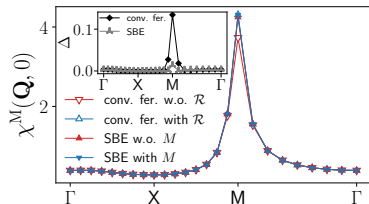
Parameters: $U = 2$, half filling

$\Rightarrow M^M$ remains finite

\Leftrightarrow Divergence in \mathcal{R}^M canceled out by w^M :

$$M_{kk'}^X(Q) = \mathcal{R}_{kk'}^X(Q) - [\lambda_k^X(Q) - 1]w^X(Q)[\lambda_{k'}^X(Q) - 1]$$

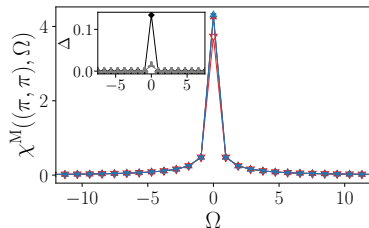
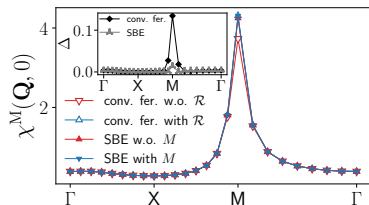
Neglecting M in SBE fRG clearly better approximation than \mathcal{R} in conv. fer. fRG at 1 loop



Parameters: $U = 2$, $T = 0.15$, half filling

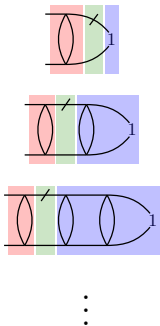
Neglecting M in SBE fRG clearly better approximation than \mathcal{R} in conv. fer. fRG at 1 loop

↔ Why does the SBE approximation induce so little loss?



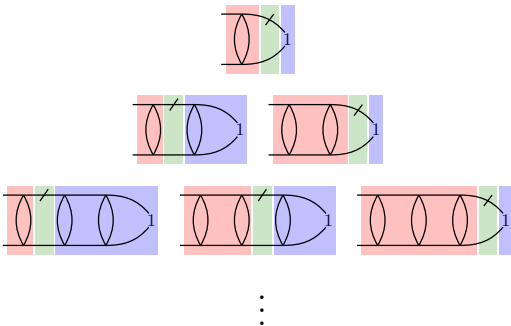
Parameters: $U = 2$, $T = 0.15$, half filling

$\partial_\Lambda \lambda^X$ in SBE



$$\partial_\Lambda \lambda_k^X(Q) = \int_p \mathcal{I}_p^X(Q) \left[\tilde{\partial}_\Lambda \Pi_p^X(Q) \right] \lambda_p^X(Q)$$

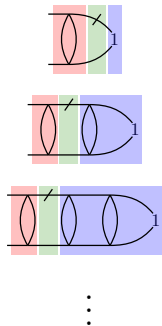
$\partial_\Lambda \lambda^X$ in SBE with M



$$\begin{aligned} \partial_\Lambda \lambda_k^X(Q) &= \int_p \mathcal{I}_{kp}^X(Q) \left[\tilde{\partial}_\Lambda \Pi_p^X(Q) \right] \lambda_p^X(Q) \\ (+\partial_\Lambda M_{kk'}^X(Q) &= \int_p \mathcal{I}_{kp}^X(Q) \left[\tilde{\partial}_\Lambda \Pi_p^X(Q) \right] \mathcal{I}_{pk'}^X(Q)) \end{aligned}$$

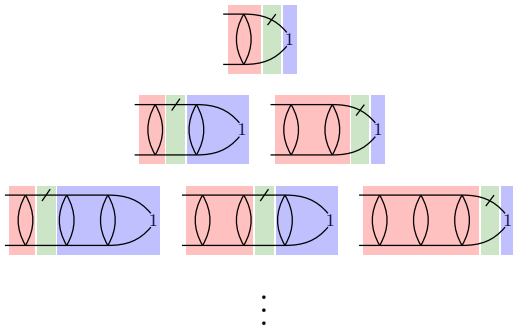
Recall: $\mathcal{I}^X \sim \Gamma^{(4)} - \lambda^X w^X \lambda^X$ and $\Pi^X \sim GG$

$\partial_\Lambda \lambda^X$ in SBEa



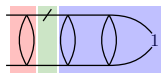
$$\partial_\Lambda \lambda_k^X(Q) = \int_p \mathcal{I}_{kp}^X(Q) \left[\tilde{\partial}_\Lambda \Pi_p^X(Q) \right] \lambda_p^X(Q)$$

$\partial_\Lambda \lambda^X$ in SBE with M

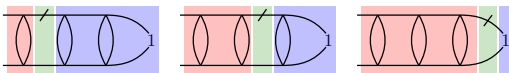
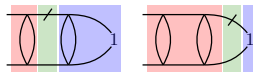


$$\begin{aligned} \partial_\Lambda \lambda_k^X(Q) &= \int_p \mathcal{I}_{kp}^X(Q) \left[\tilde{\partial}_\Lambda \Pi_p^X(Q) \right] \lambda_p^X(Q) \\ (+\partial_\Lambda M_{kk'}^X(Q) &= \int_p \mathcal{I}_{kp}^X(Q) \left[\tilde{\partial}_\Lambda \Pi_p^X(Q) \right] \mathcal{I}_{pk'}^X(Q)) \end{aligned}$$

Recall: $\mathcal{I}^X \sim \Gamma^{(4)} - \lambda^X w^X \lambda^X$ and $\Pi^X \sim GG$

$\partial_\Lambda \lambda^X$ in SBEb $\partial_\Lambda \lambda^X$ in SBEa

⋮

 $\partial_\Lambda \lambda^X$ in SBE with M 

⋮

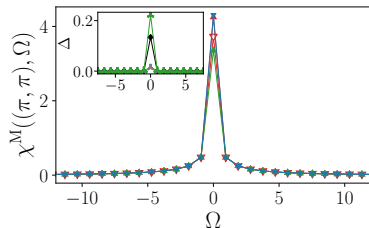
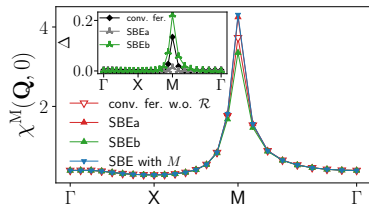
$$\partial_\Lambda \lambda_k^X(Q) = \int_p \mathcal{I}_{kp}^X(Q) \left[\tilde{\partial}_\Lambda \Pi_p^X(Q) \right] 1$$

$$\partial_\Lambda \lambda_k^X(Q) = \int_p \mathcal{I}_{kp}^X(Q) \left[\tilde{\partial}_\Lambda \Pi_p^X(Q) \right] \lambda_p^X(Q)$$

$$\begin{aligned} \partial_\Lambda \lambda_k^X(Q) &= \int_p \mathcal{I}_{kp}^X(Q) \left[\tilde{\partial}_\Lambda \Pi_p^X(Q) \right] \lambda_p^X(Q) \\ (+\partial_\Lambda M_{kk'}^X(Q) &= \int_p \mathcal{I}_{kp}^X(Q) \left[\tilde{\partial}_\Lambda \Pi_p^X(Q) \right] \mathcal{I}_{pk'}^X(Q) \end{aligned}$$

Recall: $\mathcal{I}^X \sim \Gamma^{(4)} - \lambda^X w^X \lambda^X$ and $\Pi^X \sim GG$

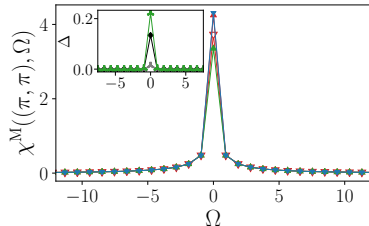
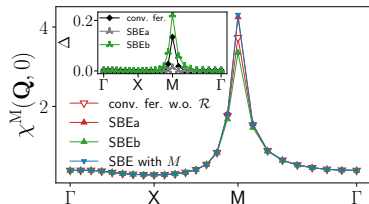
Important loss of accuracy in SBEb as compared to SBEa but SBEb restores cutoff independence...



Parameters: $U = 2$, $T = 0.15$, half filling

Important loss of accuracy in SBEb as compared to SBEa but SBEb restores cutoff independence...

- ⚠ SBEb is a self-consistent solution of parquet equations without M but SBEa inherent to fRG framework
- ⇒ Advantage of fRG formulation of SBE scheme



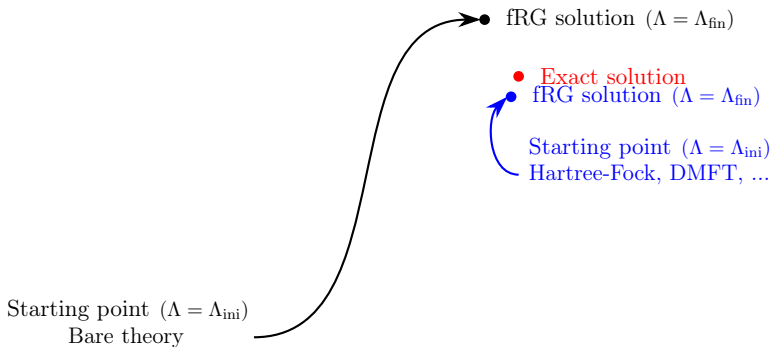
Parameters: $U = 2$, $T = 0.15$, half filling

Extension to strong couplings using DMF²RG

Section based on:

P.M. Bonetti, A. Toschi, C. Hille, S. Andergassen, and D. Vilaridi, SBE representation of the fRG for strongly interacting many-electron systems, Phys. Rev. Research 4, 013034 (2022)

Illustration of the fRG flow with/without correlated starting point:

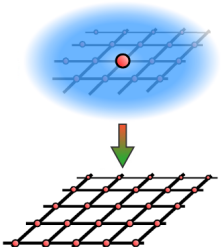


- Taranto, Andergassen, Bauer, Held, Katanin, Metzner, Rohringer, Toschi, PRL 112, 196402 (2014)
Dupuis, PRB 89, 035113 (2014)
Wentzell, Taranto, Katanin, Toschi, Andergassen, PRB 91, 045120 (2015)
Katanin, PRB 99, 115112 (2019)
Vilardi, PRB 99, 104501 (2019)

General principle of DMF²RG:

$$S^{\Lambda=\Lambda_{\text{ini}}} = - \int_0^\beta d\tau d\tau' \sum_{\sigma} c_{\sigma}^{\dagger}(\tau) \mathcal{G}_{\text{AIM}}^{-1}(\mathbf{k}, \tau - \tau')^{-1} c_{\sigma}(\tau') + S_{\text{int}}$$

$$\mathcal{G}_0^{\Lambda_{\text{ini}}}(\mathbf{k}, i\omega) = \mathcal{G}_{\text{AIM}}(i\omega)$$



$$S^{\Lambda=\Lambda_{\text{fin}}} = - \int_0^\beta d\tau d\tau' \sum_{\mathbf{k}\sigma} c_{\mathbf{k}\sigma}^{\dagger}(\tau) \mathcal{G}_{\text{latt}}^{-1}(\mathbf{k}, \tau - \tau')^{-1} c_{\mathbf{k}\sigma}(\tau') + S_{\text{int}}$$

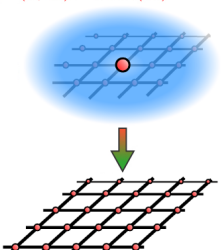
$$\mathcal{G}_0^{\Lambda_{\text{fin}}}(\mathbf{k}, i\omega) = \mathcal{G}_{\text{latt}}(\mathbf{k}, i\omega)$$

- Use the **DMFT solution as starting point** of the flow (DMF²RG = DMFT+fRG)
- Incorporate **nonlocal correlations** on top of the local ones throughout the flow

General principle of DMF²RG:

$$S^{\Lambda=\Lambda_{\text{ini}}} = - \int_0^\beta d\tau d\tau' \sum_{\sigma} c_{\sigma}^{\dagger}(\tau) \mathcal{G}_{\text{AIM}}^{-1}(\mathbf{k}, \tau - \tau')^{-1} c_{\sigma}(\tau') + S_{\text{int}}$$

$$\mathcal{G}_0^{\Lambda_{\text{ini}}}(\mathbf{k}, i\omega) = \mathcal{G}_{\text{AIM}}(i\omega)$$

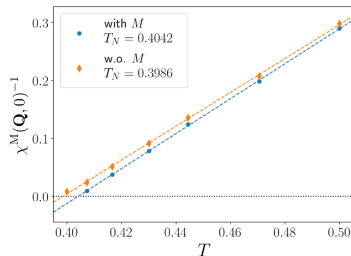


$$S^{\Lambda=\Lambda_{\text{fin}}} = - \int_0^\beta d\tau d\tau' \sum_{\mathbf{k}\sigma} c_{\mathbf{k}\sigma}^{\dagger}(\tau) \mathcal{G}_{\text{latt}}^{-1}(\mathbf{k}, \tau - \tau')^{-1} c_{\mathbf{k}\sigma}(\tau') + S_{\text{int}}$$

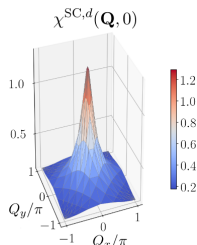
$$\mathcal{G}_0^{\Lambda_{\text{fin}}}(\mathbf{k}, i\omega) = \mathcal{G}_{\text{latt}}(\mathbf{k}, i\omega)$$

- Use the **DMFT** solution as starting point of the flow (DMF²RG = DMFT+fRG)
- Incorporate **nonlocal correlations** on top of the local ones throughout the flow

DMF²RG formulated also in the SBE scheme:



Parameters: $U = 8$, half filling



Parameters: $U = 8$, $T = 0.044$, $\Lambda \neq \Lambda_{\text{fin}}$, finite doping

Conclusion

Main conclusions of our SBE fRG study:

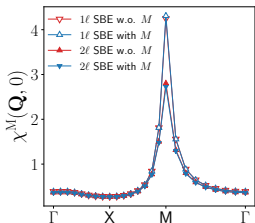
- **Rest function M negligible** in most studied cases at 1 loop, at weak and strong couplings (with DMF²RG)
- **Advantages of the SBE fRG over the conventional fermionic fRG** especially in the vicinity of the pseudo-critical transition at 1 loop

Main conclusions of our SBE fRG study:

- **Rest function M negligible** in most studied cases at 1 loop, at weak and strong couplings (with DMF²RG)
- **Advantages of the SBE fRG over the conventional fermionic fRG** especially in the vicinity of the pseudo-critical transition at 1 loop

Outlooks for the SBE fRG:

- Design a quantitative fRG approach at strong couplings
 ↪ Calculate multiloop corrections for DMF²RG in the SBE scheme
 Kugler, von Delft, PRL 120, 057403 (2018), PRB 97, 035162 (2018)
 Gievers, Walter, Ge, von Delft, Kugler, EPJB 95, 108 (2022)
- Comparison with other fRG schemes based on Hubbard-Stratonovich transf.
 ↪ Connection with Denz, Mitter, Pawłowski, Wetterich, Yamada, PRB 101, 155115 (2020)



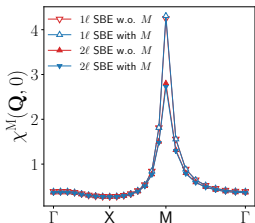
Parameters: $U = 2$, $T = 0.15$, half filling

Main conclusions of our SBE fRG study:

- **Rest function M negligible** in most studied cases at 1 loop, at weak and strong couplings (with DMF²RG)
- **Advantages of the SBE fRG over the conventional fermionic fRG** especially in the vicinity of the pseudo-critical transition at 1 loop

Outlooks for the SBE fRG:

- Design a quantitative fRG approach at strong couplings
 ↪ Calculate multiloop corrections for DMF²RG in the SBE scheme
 Kugler, von Delft, PRL 120, 057403 (2018), PRB 97, 035162 (2018)
 Gievers, Walter, Ge, von Delft, Kugler, EPJB 95, 108 (2022)
- Comparison with other fRG schemes based on Hubbard-Stratonovich transf.
 ↪ Connection with Denz, Mitter, Pawłowski, Wetterich, Yamada, PRB 101, 155115 (2020)



Parameters: $U = 2$, $T = 0.15$, half filling

See [A. Al-Eryani's talk](#) for applications to non-local interactions

Backup slides

Conventional decomposition of the 2-particle vertex $\Gamma^{(4)}$ within the fermionic fRG (Wentzell, Li, Tagliavini, Taranto, Rohringer, Held, Toschi, Andergassen, PRB 102, 085106 (2020)):

$$\phi_{kk'}^X(Q) \equiv (V - \mathcal{I}^{2\text{PI}})_{kk'}^X(Q) = \mathcal{K}^{(1)X}(Q) + \mathcal{K}_k^{(2)X}(Q) + \mathcal{K}_{k'}^{(2)X}(Q) + \mathcal{R}_{kk'}^X(Q)$$

with the high-frequency asymptotics:

$$\mathcal{K}^{(1)X}(Q) = \lim_{\nu, \nu' \rightarrow \infty} \phi_{(\mathbf{k}, \nu), (\mathbf{k}', \nu')}^X(Q)$$

$$\mathcal{K}_k^{(2)X}(Q) = \lim_{\nu' \rightarrow \infty} \phi_{\bar{k}, (\mathbf{k}', \nu')}^X(Q) - \mathcal{K}^{(1)X}(Q)$$

and \mathcal{R} the rest function

⚠ \mathcal{R} = counterpart of the multiboson exchange contributions M for the conv. fer. fRG

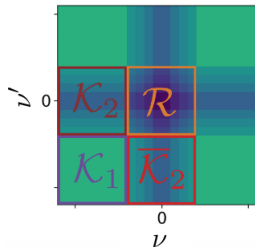


Figure adapted from C. Hille, PhD thesis (2020)

Possibility to express SBE quantities in terms of those inherent to the conventional fermionic fRG:

$$\text{Consider } \begin{cases} \phi_{kk'}^X(Q) = \lambda_k^X(Q) w^X(Q) \lambda_{k'}^X(Q) + M_{kk'}^X(Q) - U \\ \phi_{kk'}^X(Q) = \mathcal{K}^{(1)X}(Q) + \mathcal{K}_k^{(2)X}(Q) + \mathcal{K}_{k'}^{(2)X}(Q) + \mathcal{R}_{kk'}^X(Q) \end{cases}$$

$\Rightarrow w$ and λ vs \mathcal{K} functions:

$$w^X(Q) = U + \mathcal{K}^{(1)X}(Q)$$

$$\lambda_k^X(Q) = 1 + \frac{\mathcal{K}_k^{(2)X}(Q)}{w^X(Q)}$$

\Rightarrow SBE rest function M vs conv. fer. rest function \mathcal{R} :

$$M_{kk'}^X(Q) = \mathcal{R}_{kk'}^X(Q) - [\lambda_k^X(Q) - 1]w^X(Q)[\lambda_{k'}^X(Q) - 1]$$